Research Square

Preprints are preliminary reports that have not undergone peer review.
They should not be considered conclusive, used to inform clinical practice,
or referenced by the media as validated information.

Locality Spectroscopy of Quantum Statistical Information

Idrees Oreibi

idrees114af@gmail.com

Directorate of Education Babylon, Ministry of Education, Iraq, Babil

Rehab Shather Abdul Hamza

Directorate of Education Babylon, Ministry of Education, Iraq, Babil

Research Article

Keywords: quantum Fisher information, quantum statistical information, controlled noise, quantum metrology

Posted Date: September 17th, 2026

DOI: https://doi.org/10.21203/rs.3.rs-11061512/v1

License: This work is licensed under a Creative Commons Attribution 4.0 International License.
Read Full License

Additional Declarations: The authors declare no competing interests.

Locality Spectroscopy of Quantum Statistical Information

Idrees Oreibi,[1,*] Ayoub Oreibi,[2,†] and Rehab Shather Abdul Hamza[1,‡]
[1] *Directorate of Education Babylon, Ministry of Education, Iraq, Babil*
[2] *Ministry of Health, Iraq*

Where in a composite quantum system does information about an unknown parameter first become locally identifiable? We define a coordinate-invariant *locality spectrum* from rank births of reduced statistical tangents and show that controlled local noise reads out this spectrum through Fisher-information valuations. For a product regular reset satisfying the stated support-filtration injectivity assumptions, the jth elementary-symmetric Fisher volume vanishes with order $2\alpha\sum_{i\le j} d_i$; for independent flagged erasure with full-rank reduced baselines the order is $\sum_{i\le j} d_i$. At maximal mixing, local depolarization and flagged erasure obey an exact Fisher-matrix substitution. Reanalysis of public logical-qubit data provides complementary tests: direct Pauli-tangent analysis of four-qubit logical-Bell counts places 99.719% of the debiased tangent power at weight 3, with a broad finite-window 3:6 erasure/reset valuation plateau; 825,000 dual-rail Ramsey attempts verify flagged-Fisher accounting; and 10.8 million repeated-CZ outcomes expose a small but metrologically aligned correlated-noise correction. These results establish locality spectroscopy as a reproducible route from subsystem identifiability to controlled-noise response.

A multiparameter quantum state can contain statistical directions that are invisible to every small subsystem yet identifiable globally. This is distinct from asking how much Fisher information exists [1]: the structural question is *at what subsystem size each independent direction first becomes visible*. Previous work has connected erasure-tolerant metrology to code weight distributions for structured probe families [2]. Here we formulate the corresponding object directly for arbitrary differentiable multiparameter state families, make it invariant under nonsingular reparameterization, and derive noise-valuation laws for the full Fisher geometry rather than for a single scalar precision.

Let $\rho_{\boldsymbol{\theta}}$ be differentiable at $\boldsymbol{\theta}_\star$, with tangents $\Delta_\mu = \partial_{\theta_\mu}\rho|_{\boldsymbol{\theta}_\star}$. In a tensor-product orthonormal operator basis $\{B_\alpha\}$, write

$$\Delta_\mu = \sum_{\alpha\neq 0} c_{\alpha\mu} B_\alpha, \qquad C_k = \operatorname{span}\{\boldsymbol{c}_\alpha : w_\alpha \le k\}, \tag{1}$$

where w_α is support size, $R_k = \dim C_k$, and

$$d_j = \min\{k : R_k \ge j\}. \tag{2}$$

The nondecreasing list $(d_1, \ldots, d_r)$ is the *locality spectrum*. Because an invertible parameter Jacobian right-multiplies all coefficient rows, every R_k and d_j is coordinate invariant. If the relevant reduced baseline states are full rank, the definition is operational:

$$\operatorname{rank}\left(\sum_{|A|\le k} F_A\right) = R_k, \tag{3}$$

with F_A the reduced-state symmetric-logarithmic-derivative (SLD) Fisher matrix [1]. The proof follows because the kernel of F_A is exactly the set of parameter directions with zero reduced tangent; details are in the Supplemental Material [3].

Now apply the same parameter-independent one-site channel to each site. Fix a local basis with one identity element and a traceless complement. For a trace-preserving regular reset with full-rank reset state, assume uniformly on that traceless complement that $\Phi_\epsilon(X) = \epsilon^\alpha L(X) + o(\epsilon^\alpha)$, with L injective, and that the induced leading map on the associated support-graded filtration is injective. Let $F_{\mathrm{reset}}(\epsilon)$ denote the resulting Fisher matrix (or another analytic positive information metric). Cauchy–Binet positivity and a minimum-cost independent-set argument give

$$\operatorname{ord}_{\epsilon=0} e_j[F_{\mathrm{reset}}(\epsilon)] = 2\alpha \sum_{i=1}^{j} d_i. \tag{4}$$

For independent site retention p with an observed, parameter-independent erasure flag, and with every reduced baseline state entering the rank filtration full rank,

$$\operatorname{ord}_{p=0} e_j[F_{\mathrm{era}}(p)] = \sum_{i=1}^{j} d_i. \tag{5}$$

Here e_j is the jth elementary symmetric polynomial of the nonzero Fisher eigenvalues. The factor of two arises because reset suppresses tangent amplitudes before the information metric squares them, whereas flagged erasure contributes a survival probability. At a maximally mixed N-qubit operating point, weight-resolved tangent Gram matrices W_r give $F_{\mathrm{dep}}(\eta) = \sum_r \eta^{2r} W_r$ and $F_{\mathrm{era}}(p) = \sum_r p^r W_r$, hence the exact matrix identity $F_{\mathrm{dep}}(\eta) = F_{\mathrm{era}}(\eta^2)$.

We tested these statements against public experiments, separating exact source measurements from our derived analyses. First, the logical-Bell experiment of Chung *et al.* uses the $[[4,2,2]]$ code and supplies all $3^4 = 81$ local-Pauli settings [4, 5]. For the ideal family $|\Psi_\phi\rangle = (|00\rangle_L + e^{i\phi}|11\rangle_L)/\sqrt{2}$ with generator $G = IIZZ/2$, the

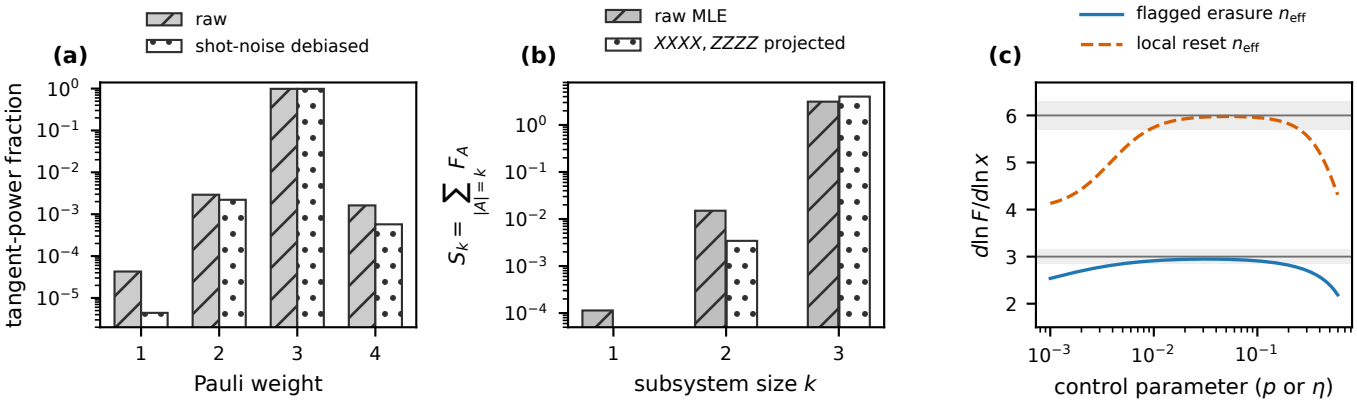


FIG. 1. **Logical-Bell locality test from public neutral-atom data.** (a) Tangent-power fractions extracted directly from the 81 local-Pauli settings of the ColdQuanta/Infleqtion dataset [4, 5], without density-matrix reconstruction. Shot-noise debiasing leaves 99.719% at Pauli weight 3. (b) A methodologically distinct $R\rho R$ reconstruction of the same counts [6] gives the sum S_k of reduced QFIs over all size-k subsystems; the weight-3 hierarchy becomes stronger after projection onto the source code stabilizers $XXXX$ and $ZZZZ$. (c) Effective logarithmic exponents for state-level flagged erasure and a computational independent local-depolarizing contraction of the projected state. The shaded bands are ±5% around 3 and 6. The reset curve is a retrospective state-level calculation, not a physical noise sweep.

tangent has eight nonzero Pauli components, all of weight 3, so its strict single-parameter locality is $d = 3$. From the deposited counts (168,386 attempted shots; 157,772 post-loss outcomes), we estimated the tangent coefficients directly through $-i\langle[P, G]\rangle$, pooling all compatible local settings. The raw weight-3 fraction is 99.5402% and the variance-subtracted value is 99.7190% [Fig. 1(a)]. In 2000 setting-wise multinomial resamples, the 2.5th percentile remains 99.20% raw and 99.38% after the same debiasing; these percentiles are stability diagnostics, not calibrated confidence bounds. A covariance-aware joint Wald test nevertheless resolves the lower-weight coefficients ($\chi^2 = 268.27$, 32 degrees of freedom, $p = 3.9 \times 10^{-39}$). Thus the *experimental* state is not a strict $d = 3$ asymptote; rather, it is overwhelmingly weight-3 over a finite practical window.

A methodologically distinct physical-state reconstruction of the same deposited counts provides the operational cross-check in Eq. (3); it is not independent evidence at the data level. Summing QFI over all subsets of exact size k gives $(S_1, S_2, S_3) = (1.13 \times 10^{-4}, 1.50 \times 10^{-2}, 3.132)$, so $S_3/(S_1 + S_2) = 208$. Projecting onto both code stabilizers gives $(0, 0.00341, 3.978)$ and a contrast of 1165 [Fig. 1(b)]. Applying the two noise maps to that projected state yields a broad finite-window realization of the predicted 1:2 valuation relation: the local effective exponent $d\ln F/d\ln p$ stays within 5% of 3 for $0.0051 \lesssim p \lesssim 0.168$, while the computational local-reset exponent stays within 5% of 6 for $0.0091 \lesssim \eta \lesssim 0.254$ [Fig. 1(c)]. At sufficiently small control parameter, the statistically resolved lower-body leakage necessarily changes the strict experimental asymptote.

The dual-rail cavity data give a complementary flagged-information test. The ideal phase family $(|01\rangle + e^{i\phi}|10\rangle)/\sqrt{2}$ has a tangent only in the XY and YX sectors and therefore strict $d = 2$. The Zenodo record of Chou *et al.* provides aggregate logical counts and erasure assignments over 11 delays and 15 phase values [7, 8], totaling 825,000 attempts (800,219 successful state preparations under the source convention). Writing $s(\phi) = P(0_L|\text{survive}, \phi)$ and $e(\phi) = P(\text{erasure}|\phi)$, the full three-outcome classical Fisher information decomposes exactly as

$$F_C = (1 - e)\frac{(s')^2}{s(1 - s)} + \frac{(e')^2}{e(1 - e)}. \tag{6}$$

First-harmonic fits to each phase sweep show that discarding the erasure branch and reporting survivor-only CFI would overstate information per successful preparation by a factor 1.162–1.209, while the explicit flag term contributes at most 6.36×10^{-4} of the full CFI [Fig. 2(a)]. Because this experiment does not sweep independent site retention, it tests flagged-Fisher accounting rather than the p^2 valuation itself.

Finally, the repeated-CZ dual-rail-gate archive [9, 10] lets us separate *erasure-flag* correlations from correlations in the surviving noise. Aggregating the nine outcomes over all 36 QST bases at ten gate depths gives 10.8 million counts. The two binary erasure indicators have $\max|\phi| = 0.00818$ and $\max I(E_1; E_2) = 4.82 \times 10^{-5}$ bits [Fig. 2(b)], even though the independently reported dephasing decomposition contains $p_{ZZ}/p_Z = 35.2\%$ at one CZ and 40.2% at three CZs. For the XY/YX phase tangent, ZZ acts trivially while ZI and IZ reverse the coherence. Comparing the measured correlated dephasing model with a product model constrained to the same one-qubit Z marginals gives a tangent-aligned relative deviation $\rho_{\text{aligned}} = 0.00378$–$0.03043$ and a phase-QFI ra-

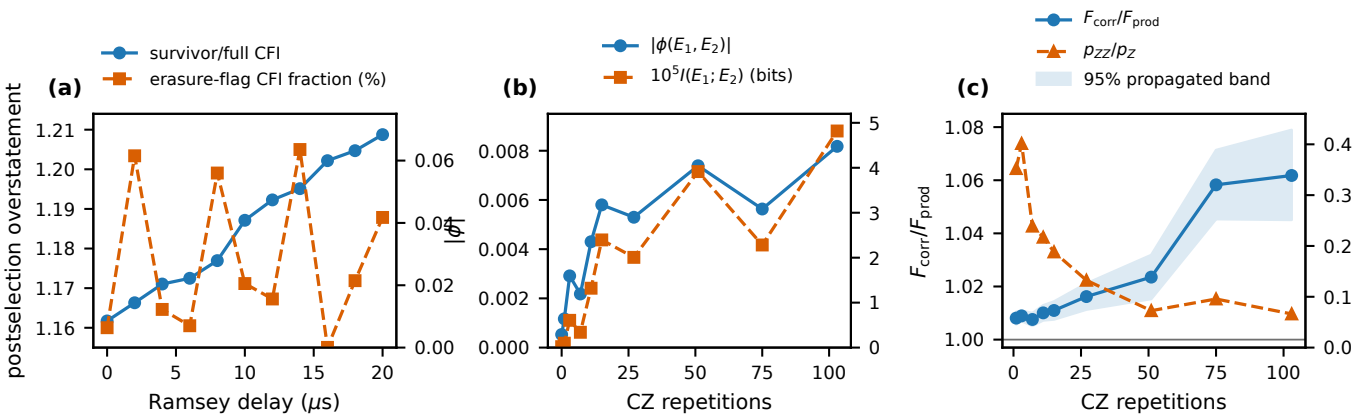


FIG. 2. **Flagged-Fisher accounting and correlated-noise diagnostics.** (a) Reanalysis of the short-time phase sweeps from the superconducting dual-rail dataset of Chou *et al.* [7, 8]. Conditioning on survivors alone overstates CFI per successful preparation by 16.2–20.9%; the explicit parameter information in the erasure flag is below 0.064% of the full flagged CFI. (b) In 10.8 million outcomes from the repeated-CZ QST dataset [9, 10], the two binary erasure flags remain weakly dependent: $\max|\phi| = 8.18 \times 10^{-3}$ and the mutual information never exceeds 4.82×10^{-5} bits per shot. (c) The same source reports a substantial correlated ZZ dephasing sector. Relative to a product channel with the same one-qubit Z marginals, its tangent-aligned phase-QFI ratio reaches 1.062; the shaded interval propagates the source-reported standard errors.

tio $F_{\mathrm{corr}}/F_{\mathrm{prod}} = 1.0076$–$1.0618$ [Fig. 2(c)]. Thus nearly independent erasure flags do not imply a product channel, and the relevance of correlated noise depends on its alignment with the metrological tangent.

The three reanalyses have deliberately different evidentiary roles. The logical-Bell data test higher-body tangent structure and finite-window valuation behavior; the Ramsey data test correct Fisher accounting with an observed erasure outcome; the repeated-CZ data test the boundary between approximately local erasure statistics and correlated surviving noise. No source implements a purpose-built $d > 1$ experiment with both a calibrated physical local-reset sweep and independent physical flagged erasure on the same state family. Such an experiment remains the cleanest direct test of Eqs. (4) and (5) under identical hardware conditions.

We thank the original experimental teams for making their data publicly available. All experimental measurements reanalyzed here were generated by the creators cited in Refs. [5, 8, 10]; no new laboratory data were generated by the present authors.

DATA AND SOFTWARE AVAILABILITY. The accompanying reproducibility package contains the author-generated code, derived tables, and figure source data selected for the reported analyses. External raw files are not redistributed; the package records exact public sources, checksums, and analysis boundaries. The superconducting-qubit inputs are the public repository records in Refs. [8, 10]. Other external sources are listed in the Supplemental Material.

COMPUTATIONAL ASSISTANCE DISCLOSURE. OpenAI ChatGPT (GPT-5.6 Sol) and the Codex Work interface were used substantively for proof exploration, literature checking, Python implementation, numerical stress tests, figure generation, and manuscript preparation during September 2026. The authors specified the research questions and assumptions and verified outputs using explicit derivations, generalized-eigenvalue checks, deterministic regression tests, bounded-perturbation tests, independent-data cross-checks, and reproducible simulations. The authors take full responsibility for the content.

* idrees114af@gmail.com
† ayouboreibi@gmail.com
‡ alamerirehab300@gmail.com

[1] S. L. Braunstein and C. M. Caves, "Statistical distance and the geometry of quantum states," Phys. Rev. Lett. **72**, 3439 (1994), doi:10.1103/PhysRevLett.72.3439.

[2] Y. Ouyang and N. Rengaswamy, "Describing quantum metrology with erasure errors using weight distributions of classical codes," Phys. Rev. A **107**, 022620 (2023), doi:10.1103/PhysRevA.107.022620.

[3] See Supplemental Material at [URL will be inserted by publisher] for proofs of the rank and valuation theorems, estimator definitions, resampling and covariance calculations, reduced-state QFI details, finite-window exponent analysis, dual-rail Fisher accounting, correlated-noise diagnostics, and source-data provenance.

[4] W. C. Chung, D. C. Cole, P. Gokhale, *et al.*, "Fault-tolerant operation and materials science with neutral atom logical qubits," npj Quantum Inf. **11**, 193 (2025), doi:10.1038/s41534-025-01095-w.

[5] ColdQuanta, Inc., DBA Infleqtion, "Experimental Data for 'Fault-Tolerant Operation and Materials Science with Neutral Atom Logical Qubits'," Zenodo, version v2 (2025), doi:10.5281/zenodo.15427685.

[6] Z. Hradil, "Quantum-state estimation," Phys. Rev. A **55**, R1561 (1997), doi:10.1103/PhysRevA.55.R1561.

[7] K. S. Chou, T. Shemma, H. McCarrick, *et al.*, "A superconducting dual-rail cavity qubit with erasure-detected logical measurements," Nat. Phys. **20**, 1454 (2024), doi:10.1038/s41567-024-02539-4.

[8] K. S. Chou, "Datasets for 'A superconducting dual-rail cavity qubit with erasure-detected logical measurements'," Zenodo, version v1 (2024), doi:10.5281/zenodo.11099521.

[9] D-Wave Quantum Inc., "An entangling gate for dual-rail erasure qubits," Nature **656**, 47 (2026), doi:10.1038/s41586-026-10822-y.

[10] D-Wave Quantum Team, "Data for: An entangling gate for dual-rail erasure qubits," Zenodo (2026), doi:10.5281/zenodo.20433754.